

Numerical prediction of jet behavior of thermal vapor compressor

K.M. Yang^a, H.M. Lee^a, H.H. Jung^{b*}

^aGraduate School, Korea Maritime University, Busan, 606-791, Korea

^bDivision of Mechanical and Information Engineering, Korea Maritime University, Busan, 606-791, Korea
Tel. +82 (51) 410-4362; Fax +82 (51) 405-4790; email: junghh@hhu.ac.kr

Received 31 November 2010; Accepted in revised form 2 May 2011

ABSTRACT

In the present study, Fluent 6.3, CFD code was applied to study the jet behavior inside the thermal vapor compressor. The effects of back pressure on the entrainment ratios and the jet behavior were investigated. It was revealed that the effect of the back pressures was due to the air curtain effect of the primary jet. The entrainment rate was linearly dependent on the distance from the nozzle exit. The displacement effect by the boundary layer thickness could be considered to be negligible. The abrupt change in the wall static pressure at the mixing tube or the throat could be used as the criteria for well operation and well design.

Keywords: Numerical prediction; Thermal vapor compressor; Jet

1. Introduction

Thermal vapor compressor is the steam ejector. The steam ejector consists of a nozzle, a mixing chamber, and a diffuser. A jet ejected from a nozzle is called a motive fluid or a primary fluid, and an entrained fluid is called a secondary fluid. Although they have disadvantages in terms of efficiency, steam ejectors seldom break down and are able to carry a large capacity of fluid.

Previous studies on ejectors have been concerned with the theories of one-dimensional gas dynamics. Keenan and Neumann [1] developed a one-dimensional model of air ejectors. They confirmed that their theoretical analysis results were consistent with experimental results by using continuity equation, momentum equation, and energy equation. Nicholas et al. [2] proposed appropriate shapes of motive nozzles by conducting experimental studies. Matsuo et al. [3,4] investigated vacuum characteristics of ejectors over a range of primary nozzle Mach numbers

and throat area ratio. They reveal that optimum area ratio exists for each Mach number and that performance curves could be classified into five groups. Dutton and Carrol [5] conducted a study concerned with choking conditions and the performance of ejectors by applying a one-dimensional constant sectional-area ejector model with respect to the performance improvement of ejectors. The results of this study revealed that choking conditions are largely dependent upon the temperature ratio and specific heat ratio of a primary flow and a secondary flow.

Kim et al. [6] carried out numerical analysis to investigate the effect of nozzle curvature on the critical flows. They found that the discharge coefficient was very sensitive to the curvature radius of critical nozzle, leading to the peak discharge coefficient at various radii. Park and Kwon [7] investigated the ejector jets focusing on its geometrical parameters that effect on thrust performance by both experimental and numerical method. They expected that the influence of mixing duct length of ejector was helpful in a thrust performance.

* Corresponding author.

Park et al. [8] designed a TVC (thermal vapor compressor) accurately in a three-stage MED (multi-effect desalination) using a numerical analysis method. They verified the performances of TVC which was installed in a MED pilot plant experimentally. They reported that the results of the numerical and experimental studies showed good agreements. By performing a numerical analysis applying ejectors to refrigeration systems, Yu and Li [9] described a novel regenerative ejector refrigeration system using the grade thermal energy, such as solar energy and waste heat. They showed that simulation results revealed that the coefficient of performance increased by 17.8%. Rusly et al. [10] conducted a flow test which passed through a R141b ejector. The effect of ejector structure was investigated using a numerical analysis method, and the results of CFD (computational fluid dynamics) were proven with experimental data. Ji et al. [11] developed a numerical model to analyze a single effect thermal vapor compression desalination system. They found that the system performance decreased when the intake seawater temperature differs from the design values and that better system performance could be obtained by adjusting mass flow of cooling water and that decreasing the cooling water flow rate to values lower than the design value could lead to a better performance when the intake sea water temperature was lower than the design value. Kamali et al. [12] summarized the MED-TVC technique associated with the state of the art of modern desalination. Additionally they simulated all type of evaporation processes. Du et al. [13] conducted performance analyses of water and power in a combined power generation system where TVC was installed. As a result, the effect of changes in steam extraction positions in relation to evaporators on jet coefficients was proved. Ji et al. [14] investigated the flow inside of TVC in a MED system using CFD. They got the effect of the angle of the converging duct on the performance of TVC and concluded that the ejector with a converging duct angle 1° had the best performance.

In this paper, the CFD technique is used to get the effect of the discharge pressures on the entrainment ratio. The manner in which the jet behavior and flow structures influence the TVC performance is discussed. The study examines the effect of the mixing tube on the entrainment ratio of TVC.

2. Theoretical background

2.1. Performance of TVC

MED with TVC is the most efficient of the thermal desalination systems. TVC causes the steam from the last effect of MED to be re-used as a heat source for the first effect by mixing it with high-pressure steam. The performance of MED is represented by GOR (gained output ratio), which is defined by the ratio of gross fresh water production to the motive steam supplied. GOR

is directly related to the entrainment ratio (R_m) of TVC, which is defined by the ratio of the mass flow of secondary flow to the mass flow of the primary fluid. GOR and R_m are related by the following relation, as shown in Eq. (1).

$$\text{GOR} = n \times (1 + R_m) \quad (1)$$

where GOR and R_m are expressed as shown Eq. (2) and Eq. (3) respectively.

$$\text{GOR} \equiv \frac{\dot{m}_t (\approx n \times \dot{m}_d)}{\dot{m}_p} = \frac{\dot{m}_t \{ \approx n \times (\dot{m}_p + \dot{m}_s) \}}{\dot{m}_p} \quad (2)$$

$$R_m = \frac{\dot{m}_s}{\dot{m}_p} \quad (3)$$

Accurate design and prediction of TVC performance are very important to the reliability of sea water desalination systems. Fig. 1 illustrates a schematic view of pressure and velocity variations in the typical TVC based on one-dimensional gas dynamics. A high-pressure steam is expanded and accelerated through a nozzle from subsonic to supersonic velocity (i), and is ejected from the nozzle (ii). The expanding jet from the nozzle exit brings the pressure of the mixing chamber and the whole MED system to the vacuum state. Mixing begins at the interface between the primary fluid and the secondary fluid. Due to the momentum exchange between two fluids, the jet velocity retards. Through this mixing process, the secondary fluid is accelerated while the major flow is decelerated (iii). In the mixing chamber, the primary and the secondary fluids mix more in the confined wall, and static pressure is maintained until they reach the throat (iv). The supersonic velocity at the downstream of the mixing chamber results in a normal shock in the irreversible process (v). Downstream pressure of the shock wave, P_2 becomes almost two times of the upstream pressure P_1 and velocity V_2 reduces suddenly as shown in Eq. (4) and Eq. (5). This shock compresses a fluid, and velocity slows down from supersonic to subsonic (vi).

$$P_2 = \frac{1}{k+1} [2\rho_1 V_1^2 - (k-1)P_1] \quad (4)$$

$$V_2 = V_1 - \frac{P_2 - P_1}{\rho_1 V_1} \quad (5)$$

2.2. Numerical method

The flow inside TVC changes from subsonic to supersonic velocity in the axi-symmetric coordinate. The grid systems were created by Gambit, and Fluent 6.2 was used for the flow analysis. The grids were concentrated near the walls, where important phenomena were expected to occur. The flow inside the TVC was assumed to be

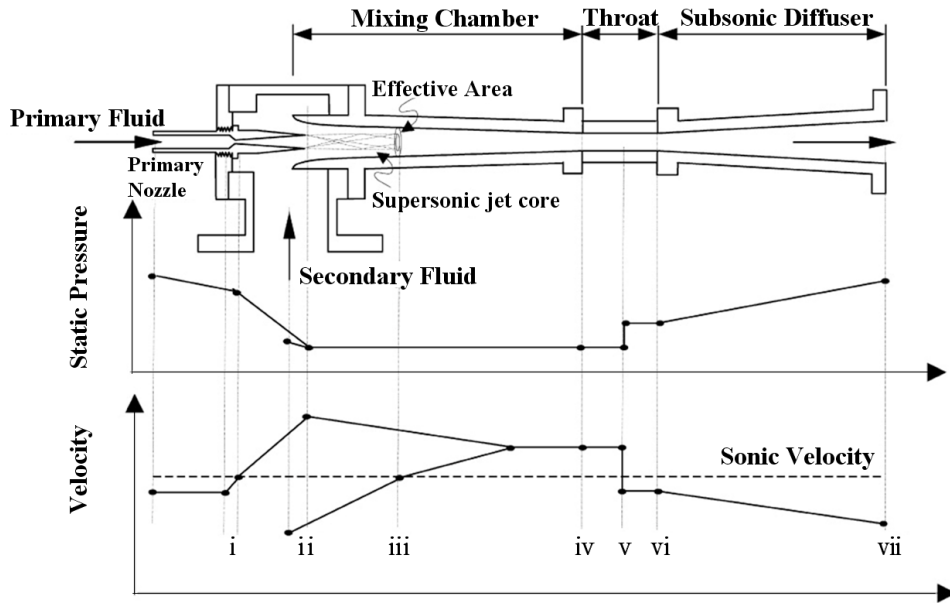


Fig. 1. Schematic view and the variation of steam pressure and velocity along a TVC [15].

compressible and transonic. The turbulent flow was assumed and “Realizable $k-\epsilon$ Model” was adopted. This is an improved version of the “Standard $k-\epsilon$ Model.” “Realizable $k-\epsilon$ Model” could predict the diffusion of jets accurately. Standard wall functions were applied to the walls. The primary and secondary streams were regarded as ideal gases. Non-linear governing equations were discretized into linear equations using the finite volume method, and calculated by the coupled implicit solver. Pressure boundary conditions were applied to the motive steam section, the suction steam section, and the discharge steam section, and their corresponding values appear in Table 1.

3. Results and discussion

The accuracy of the numerical analyses is dependent upon the number of grids. Though more grids lead to more accurate numerical results, the grids are limited by the capacity of the computer and the computing time. To get the appropriate grid system, a grid test was done by changing the grid system in 3 regions — the inside nozzle, the suction region and the converging and diverging duct.

Table 1
Boundary conditions

Boundary	Pressure (atm)
Motive regions	2.66
Suction region	0.163
Discharge region	0.26, 0.28, 0.3, 0.31, 0.32

Fig. 2 illustrates the effect of grid systems on the mass flow rates of the motive steam and the suction steam. The numbers in Fig. 2 means grid systems at each region. Although the mass flow of motive steam was insensitive to the number of grids, mass flow of suction steam was sensitive to the number of grids in the converging/diverging ducts. More grids were concentrated at the boundary layer and especially at the mixing layer by using the non uniform grid to get the accurate solutions. Some distorted grids (sudden changes of grid sizes and

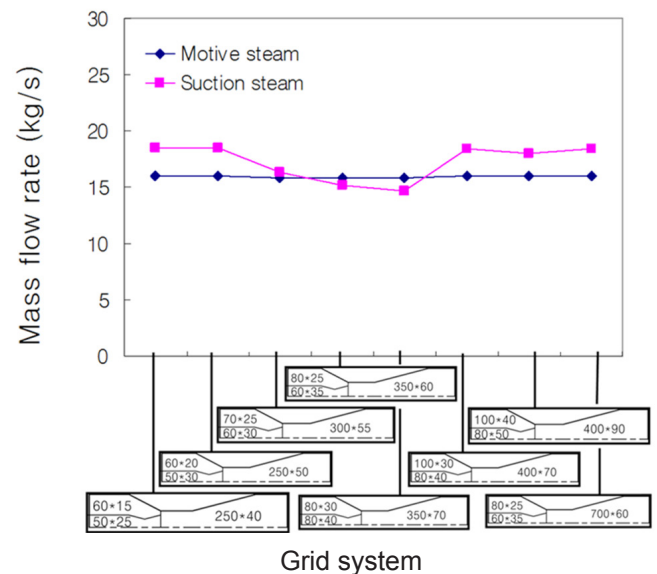
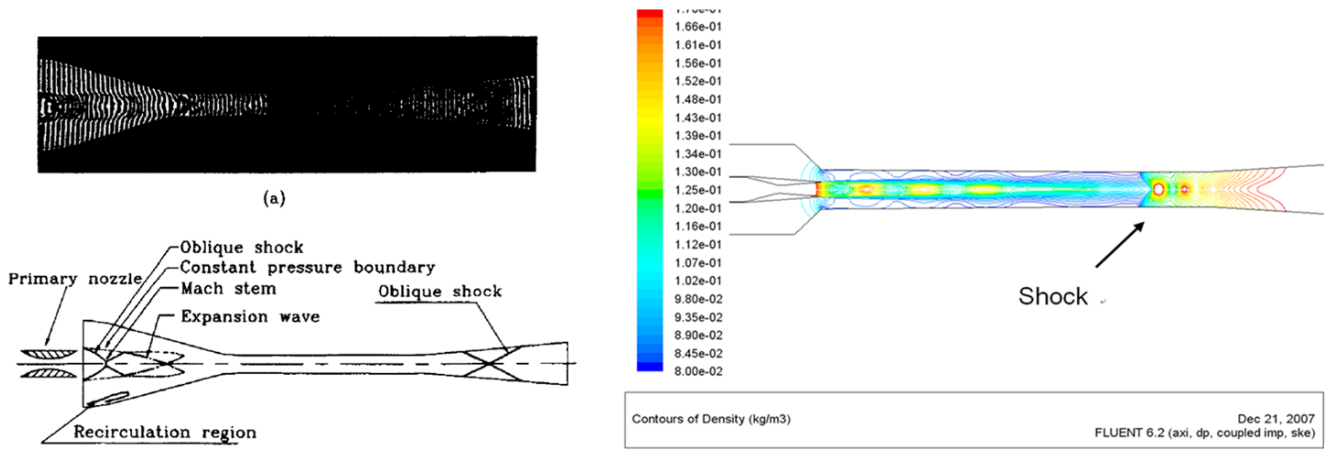


Fig. 2. Grid refinement test.



(a) By Chen and Sun’s holographic interferogram

(b) Density patterns by numerical calculation

Fig. 3. Comparison of wave pattern.

the aspect ratio between the neighboring grids) made the inaccurate solutions. For grids more than 400×70 in the converging/diverging duct, the mass flow rate of the suction steam remains almost constant. In present study, the grid system with 400×70 grids in converging/diverging ducts was selected for the simulation.

In Fig. 3, Chen and Sun’s wave pattern [16] was compared with the density contours after the primary nozzle. The nozzle outlet Mach number is 2.5. The flow structure inside the TVC was revealed using an optical flow-visualization method. The holographic interferogram of an air-ejector shows that diamond-like shock and expansion waves are repeatedly generated at the exit of the nozzle. Fig. 3 reveals that the shape of constant density lines shows a series of beads. The present computational approach simulates the shock and expansion waves accurately inside the TVC. The dramatic density change at the downstream was thought to be normal shock.

Fig. 4 shows stream-lines of a primary fluid and a secondary fluid. This figure shows that the primary fluid and the secondary fluid are moving toward the downstream in a manner almost parallel to the outer wall despite the presence of the density gradient, and that the density gradient does not disturb the flows. It was near normal shock where the flows were affected by the presence of density gradient.

Discharge pressures were changed in order to investigate the effect of back pressure on the entrainment ratio and the flow structure inside TVC. The effect of back pressure on the entrainment ratio is shown in Fig. 5. Consistent with previous studies, the entrainment ratio was predicted as almost constant below the MDP (maximum discharge pressure).

To investigate the effect of discharge pressures on the entrainment ratios, the gradients of the axial velocities are plotted in Fig. 6. By plotting the gradients of the axial

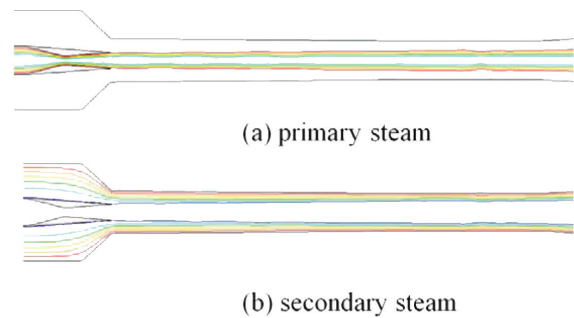


Fig. 4. Stream lines of primary and secondary steams.

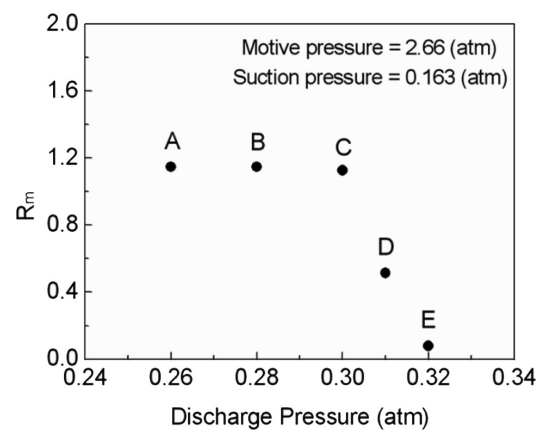


Fig. 5. Effect of suction pressures on entrainment ratio.

velocity, the development of boundary layers (thin shear layer) along the walls and the spreading of the mixing layer (thick shear layer) generated at the interface of the jet and jet behaviors could be identified. Fig. 6 shows that due to the entrainment of the secondary fluid, the

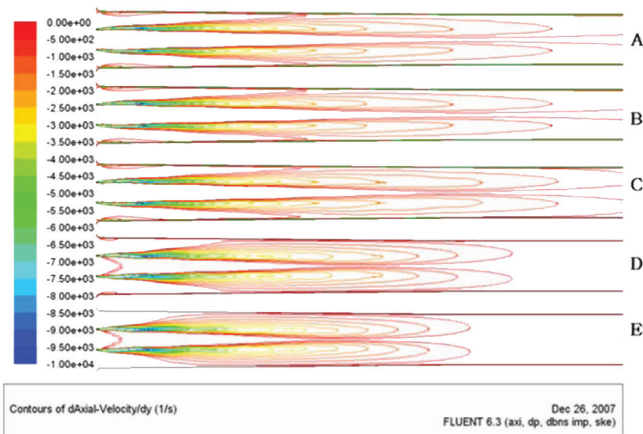


Fig. 6. Jet behaviors of the motive steam due to the discharge pressure.

thickness of the mixing layer increases. Finally, the mixing layer reaches the wall, and the entire flow field is filled out by the jet. The mixing layer has a conical shape. The boundary layers are developing along the walls by the flow of secondary fluid. The developing boundary layer thickness inside TVC is different when it is compared with the other internal flow. The boundary layer develops on the outer wall, and the boundary layer thickness is increased. As the jet entrains the surrounding fluid, the flow rate of secondary fluid between the mixing layer and the boundary layer becomes smaller and smaller, and the thickness of boundary layer becomes thinner and thinner. Finally, the boundary layer disappears, which means that the suction steam is entrained into the jet completely.

As shown in Fig. 5, the entrainment ratios on the points A, B, C where discharge pressures were under MDP were almost constant, and the mass flow of the motive steam and the secondary fluid inside TVC became nearly constant. This means that the jet completely fills the flow field of the mixing tube section. The jet behaves like an air curtain, which prevents the discharge pressures from affecting the secondary fluid at the upstream. At the points A, B, and C the interface area where the entrainment occurs is almost constant; therefore, the entrainment ratio and the secondary fluid flow rate are also constant.

At the points D and E (points more than MDP), discharge pressures block the jet flow, shortening the length of the jet and spreading it. The interface where the jet entrains the secondary fluid was decreased in a linear manner, to the extent of the reduced length of the jet. This means that the entrainment rate might be linearly dependent on the length of the jet (the axial distance from the nozzle exit). Rajarathan [17] reported that the volumetric flux at any axial direction flow was linearly dependent on the axial distance from the nozzle exit. It can thus be seen that the spreading angle of the mixing layer into the secondary fluid was bigger than the spreading angle into the jet core. Fig. 6 shows that at the upstream, where the mixing layer meets the wall, the boundary layer thickness disappears. This means that it is not necessary to consider the displacement thickness by the boundary layer in the design of TVC.

To get the appropriate shape for TVC, the geometric data of the mixing tube and the throat were varied, as shown in Fig. 7. The representative TVC geometric data and operating conditions can be seen in Table 2. In order to determine the effect of the length of the mixing tube on performance, the length of the mixed tube was changed in the range of $\pm 10\%$, while the total length of TVC and other geometric parameters were fixed. The effect of the length of a mixed tube on the mass flow of motive and the suction steam is compared in Fig. 8. Though the length of a mixing tube was increased, the mass flow of motive steam remained constant. However, when the length of the mixed tube was 7425 mm (inappropriate design) the suction steam flow rate was less than in the other cases.

The static pressure distributions along the wall are displayed in Fig. 9. Also, in this figure the positions of constant area (throat) are plotted. When the length of a mixed area was 7425 mm (inappropriate design), the wall

Table 2
Typical geometric data of TVC and operating conditions

Converging duct × mixing tube × diffuser	Operating pressures (atm)		
	Motives	Suction	Discharge
3375.4 × 6750 × 9875.6	2.66	0.163	0.3

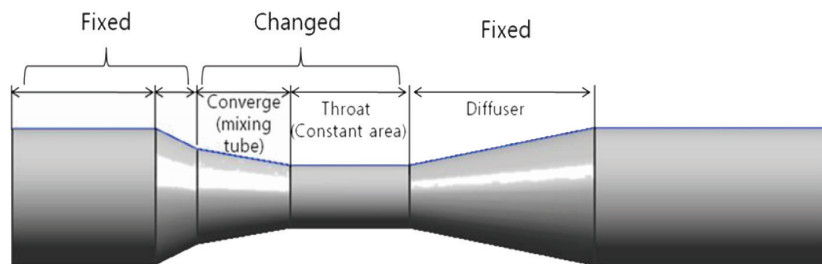


Fig. 7. Schematic view of outside contours of TVC and the definition of geometry.

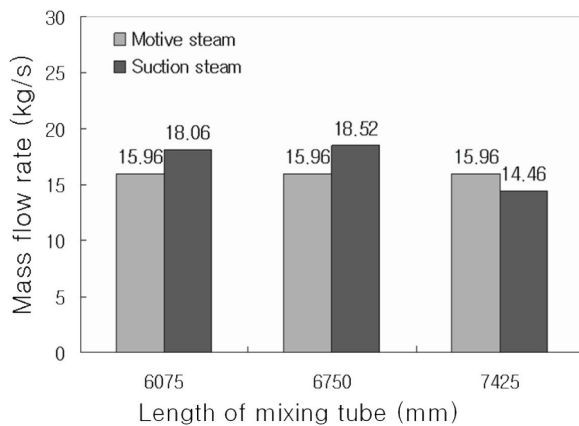


Fig. 8. Effect of mixing tube on mass flow rates.

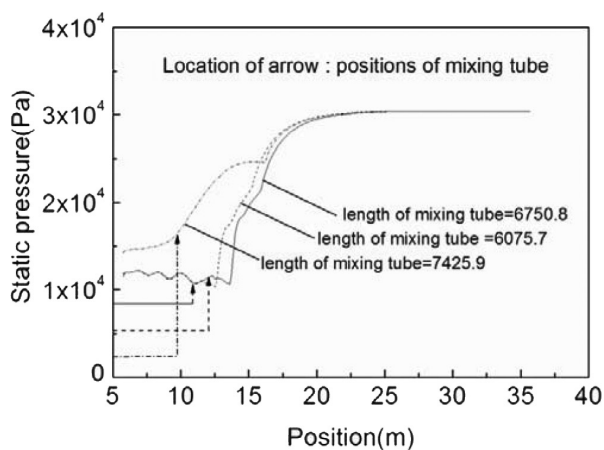


Fig. 9. Distribution of static pressure along the wall of TVC.

pressure was about 2 times higher than the appropriate cases at the mixing tube and the throat. These changes of the wall static pressure at the mixing tube could be used as indicators of the design criterion. When the design of the shape was appropriate (length of mixed area: 6750, 6075), the static pressure was monotonously increased along the wall and changed steeply. A greater increase in pressure led to a decrease of suction steam in the mixing tube and a lower mixing rate of suction steam. However, when design was inappropriate, the static pressure in the mixed area remained high. This was due to the effect of the converging duct angle on the entrainment ratio.

4. Conclusions

In this study, the axial symmetry flow inside TVC, which is applied to MED seawater desalination equipment, was analyzed using Fluent 6.2. The flow was assumed to be a compressible turbulent flow, and pressure boundary conditions were applied to it. The results of the

calculation revealed that back pressure affects the performance of TVC; furthermore, if back pressure is smaller than MDP, the entrainment ratio is constant regardless of back pressure, and the flow structure of the jets inside TVC remains the same. This effect could be likened to the primary steam acting as an air curtain, which causes the state of the suction steam to remain independent of the back pressures.

It is not necessary to consider displacement thickness in the design of TVC. The mixing layers of jets were widely spread into the secondary fluid, and the thickness of the mixed layers was changed in a linear manner. The entrainment ratio and the entrain rate could be calculated based on the linearly relation of the distance from the nozzle exit. The numerical analysis could be used as a design supplement method when designing a TVC.

Symbols

GOR	—	Gain output ratio
k	—	Specific heat ratio
\dot{m}_a	—	Mass flow rate of discharge steam, kg/s
\dot{m}_p	—	Mass flow rate of primary stream, kg/s
\dot{m}_s	—	Mass flow rate of suction stream, kg/s
\dot{m}_t	—	Total mass flow rate of, kg/
n	—	Number of effects
R_m	—	Entrainment ratio (see Eq. (3))
P	—	Pressure, Pa
V	—	Velocity, m/s
ρ	—	Density, kg/m ³

Subscripts

- Upstream of the shock
- Downstream of the shock

Acknowledgments

This study was supported by the Desalination B.G. (Water) Research Center of Doosan Heavy Industries and Construction at Dubai, and the center for seawater Desalination Plant (SeaHero) of Gwangju Institute of Science and Technology. We want to thank to all those with whom we have collaborated.

References

- [1] J.H. Keenan, E.P. Neumann and F. Lustwerk, An investigation of ejector design by analysis and experiment, *J. Appl. Mechanics*, 17 (1950) 299–309.
- [2] T.M. Nicholas, A.K. Narayana and A.E. Muthunayagam, Mixing pressure-rise parameter for effect of nozzle geometry in diffuser-ejector, *J. Propulsion Powers*, 12 (1995) 431–433.
- [3] K. Matsuo, K. Sasaguchi, K. Tasaki and H. Mochizuki, Investigation of supersonic air ejector, Part1 Performance in the case of zero-secondary flow, *Bull. JSME, Ser. B*, 24 (1995) 2090–2097.
- [4] K. Matsuo, K. Sasaguchi, K. Tasaki and H. Mochizuki, Investigation of supersonic air ejector, Part 2. Effects of throat-area-ratio on ejector performance, *Bull. JSME, Ser. B*, 25 (1982) 1898–1905.

- [5] J.C. Dutton and B.F. Carrol, Limitation of ejector performance due to exit choking, *J. Fluids Eng.*, 110 (1988) 91–93.
- [6] J.H. Kim, H.D. Kim and G.A. Park, Effect of the nozzle curvature on critical flows, 2002 Proc. Turbo-machinery R&D, 2002, pp. 331–336.
- [7] G.H. Park and S.J. Kwon, Internal flow properties and thrust characteristics of axi-symmetric annular bell type ejector-jet, Proc. 2007 Spring Meeting, Korean Society of Computational Fluids Engineering, 2007, pp. 166–170.
- [8] I.S. Park, S.M. Park and J.S. Ha, Design and application of thermal vapor compressor for multi-effect desalination plant, *Desalination*, 182 (2005) 199–208.
- [9] J. Yu and Y. Li, A theoretical study of a novel regenerative ejector refrigeration cycle, *Int. J. Refrig.*, 30 (2007) 464–470.
- [10] E. Rusly, A. Lu, W.W.S. Charters, A. Ooi and K. Phiantong, Ejector CFD modeling with real gas model, Mechanical Engineering Network of Thailand the 16th Conference, 2002, pp. 150–155.
- [11] J. Ji, R. Wang, L. Li and H. Ni, Simulation and analysis of a single-effect thermal vapor-compression desalination system at variable operation conditions, *Chem. Eng. Technol.*, 30 (2007) 1633–1641.
- [12] R.K. Kamali, A. Abbassi and S.A. Sadough Vanini, A simulation model and parametric study of MED–TVC process, *Desalination*, 235 (2009) 340–351.
- [13] Y. Du, X. Liu, S. Shen, W. Chen and D. Liu, Performance analysis of water and power cogeneration system with thermal vapor compressor, Power and Energy Engineering Conference (APPEEC), 2010 Asia-Pacific, 10.1109/APPEEC.2010.5449114.
- [14] M.K. Ji, T. Utomo, J.S. Woo, H.M. Jeong and H.S. Chung, CFD investigation on the flow structure inside thermo vapor compressor, *Int. J. Energy Res.*, 35 (2010) 2694–2702.
- [15] T. Sriveerakul and S. Aphornratana, Performance prediction of steam ejector using computational fluid dynamics: Part 1 Validation of the CFD results, *Int. J. Thermal Sci.*, 46 (2007) 812–822.
- [16] Y. Chen and C. Sun, Experimental study of the performance characteristics of steam-ejector refrigeration system, *Exp. Thermal Fluid Sci.*, 15 (1997) 384–394.
- [17] N. Rajaratnam, Turbulent mixing and diffusion of jets, in *Encyclopedia of Fluid Mechanics*, Gulf Publishing Co., Houston, 2 (1986) 391–405.